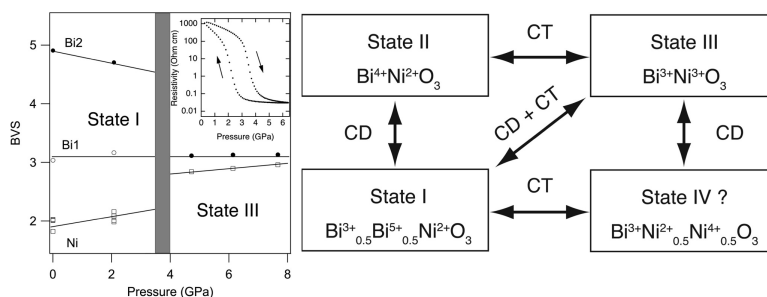


Pressure-Induced Intermetallic Valence Transition in BiNiO

Masaki Azuma, Sandra Carlsson, Jennifer Rodgers, Matthew G. Tucker, Masahiko Tsujimoto, Shintaro Ishiwata, Seiji Isoda, Yuichi Shimakawa, Mikio Takano, and J. Paul Attfield

J. Am. Chem. Soc., **2007**, 129 (46), 14433-14436 • DOI: 10.1021/ja074880u • Publication Date (Web): 31 October 2007

Downloaded from <http://pubs.acs.org> on February 13, 2009



More About This Article

Additional resources and features associated with this article are available within the HTML version:

- Supporting Information
- Links to the 4 articles that cite this article, as of the time of this article download
- Access to high resolution figures
- Links to articles and content related to this article
- Copyright permission to reproduce figures and/or text from this article

[View the Full Text HTML](#)

Pressure-Induced Intermetallic Valence Transition in BiNiO₃Masaki Azuma,^{*,†} Sandra Carlsson,[‡] Jennifer Rodgers,[‡] Matthew G. Tucker,[§] Masahiko Tsujimoto,[†] Shintaro Ishiwata,^{†,‡,‡} Seiji Isoda,[†] Yuichi Shimakawa,[†] Mikio Takano,[†] and J. Paul Attfield[‡]

Contribution from the Institute for Chemical Research, Kyoto University, Uji, Kyoto-fu 611-0011, Japan, Centre for Science at Extreme Conditions and School of Chemistry, University of Edinburgh, Mayfield Road, Edinburgh, EH9 3JZ, United Kingdom, and ISIS Facility, Rutherford Appleton Laboratory, Chilton, Didcot OX11 0QX, United Kingdom

Received July 17, 2007; E-mail: masaki@scl.kyoto-u.ac.jp

Abstract: The valence state change of BiNiO₃ perovskite under pressure has been investigated by a powder neutron diffraction study and electronic-state calculations. At ambient pressure, BiNiO₃ has the unusual charge distribution Bi³⁺_{0.5}Bi⁵⁺_{0.5}Ni²⁺O₃ with ordering of Bi³⁺ and Bi⁵⁺ charges on the A sites of a highly distorted perovskite structure. High-pressure neutron diffraction measurements and bond valence sum calculations show that the pressure-induced melting of the charge disproportionated state leads to a simultaneous charge transfer from Ni to Bi, so that the high-pressure phase is metallic Bi³⁺Ni³⁺O₃. This unprecedented charge transfer between A and B site cations coupled to electronic instabilities at both sites leads to a variety of ground states, and it is predicted that a Ni-charge disproportionated state should also be observable.

1. Introduction

Charge ordering in oxides,¹ drives many important phenomena such as the Verwey transition of Fe₃O₄ and ferroelectricity in LuFe₂O₄.² The melting of charge order often leads to exotic conducting phenomena near the insulator to metal boundary, such as colossal magnetoresistance in manganites (e.g., La_{0.5}-Ca_{0.5}MnO₃)³ and superconductivity in K- and Pb-doped Ba-BiO₃.^{4,5} Disproportionation of Bi⁴⁺ into Bi³⁺ and Bi⁵⁺ occurs at the B-sites of BaBiO₃ (BaBi³⁺_{0.5}Bi⁵⁺_{0.5}O₃)⁶ and, when suppressed by doping of K for Ba or Pb for Bi, leads to superconductivity. Similar disproportionations of high transition-metal valence states are also known in CaFeO₃ (CaFe³⁺_{0.5}Fe⁵⁺_{0.5}O₃)⁷ and RNiO₃ (RNi²⁺_{0.5}Ni⁴⁺_{0.5}O₃, for R = Y, Pr–Lu), although the observed charge separations are smaller than expected from the ideal formulas shown.^{1,8–11} Bismuth transition-metal oxide

perovskites¹² such as BiFeO₃¹³ can combine magnetic and ferroelectric functionalities, as the off-center displacements of the A-site (ideally 12-coordinate) Bi³⁺ can stabilize a ferroelectric distortion while the B-site (octahedrally coordinated) transition-metal spins order magnetically. High pressure and temperature conditions have recently been used to stabilize BiCrO₃,¹⁴ BiCoO₃,¹⁵ BiMnO₃,¹⁶ and Bi₂NiMnO₆,¹⁷ all containing Bi³⁺, but BiNiO₃ was found to have a centrosymmetric triclinic perovskite structure containing two inequivalent Bi and four Ni sites.¹⁸ Bond valence sum (BVS) calculations,¹⁹ based on the metal oxygen distances from a synchrotron X-ray powder diffraction study, revealed that the charge distribution was Bi³⁺_{0.5}Bi⁵⁺_{0.5}Ni²⁺O₃. The Ni²⁺ state was confirmed by photoemission and X-ray absorption experiments.²⁰

[†] Kyoto University.[‡] University of Edinburgh.[§] Rutherford Appleton Laboratory.^{*} Current address: Multiferroics Project, ERATO, Japan Science and Technology Agency, AIST Tsukuba Central 4, Tsukuba, Ibaraki 305-8562, Japan.

- Attfield, J. P. *Solid State Sci.* **2006**, *8*, 861–867.
- Ikeda, N.; Ohsumi, H.; Ohwada, K.; Ishii, K.; Inami, T.; Kakurai, K.; Murakami, Y.; Yoshii, K.; Mori, S.; Horibe, Y.; Kito, H. *Nature* **2005**, *436*, 1136–1138.
- Radaelli, P. G.; Cox, D. E.; Marezio, M.; Cheong, S.-W. *Phys. Rev. B* **1997**, *55*, 3015–3023.
- Cava, R. J.; Batlogg, J. B.; Krajewski, J. J.; Farrow, R.; Rupp, L. W.; White, A. E.; Short, K.; Peck, W. F.; Kometani, T. *Nature* **1988**, *332*, 814–816.
- Sleight, A. W.; Gillson, J. L.; Bierstedt, P. E. *Solid State Commun.* **1975**, *17*, 27–28.
- Cox, D. E.; Sleight, A. W. *Acta Crystallogr., Sect. B* **1979**, *35*, 1–10.
- Takano, M.; Nakanishi, N.; Takeda, Y.; Naka, S.; Takada, T. *Mater. Res. Bull.* **1977**, *12*, 923–928.
- Woodward, P. M.; Cox, D. E.; Moshopoulou, E.; Sleight, A. W.; Morimoto, S. *Phys. Rev. B* **2000**, *62*, 844–855.
- Takeda, T.; Kanno, R.; Kawamoto, Y.; Takano, M.; Kawasaki, S.; Kamiyama, T.; Izumi, F. *Solid State Sci.* **2000**, *2*, 673–687.

- Alonso, J. A.; García-Muñoz, J. L.; Fernández-Díaz, M. T.; Aranda, M. A. G.; Martínez-Lope, M. J.; Casais, M. T. *Phys. Rev. Lett.* **1999**, *82*, 3871–3874.
- Saito, T.; Azuma, M.; Nishibori, E.; Takata, M.; Sakata, M.; Nakayama, N.; Arima, T.; Kimura, T.; Urano, C.; Takano, M. *Physica B* **2003**, *329*, 866–867.
- Azuma, M.; Niitaka, S.; Belik, A. A.; Ishiwata, S.; Saito, T.; Takata, K.; Yamada, I.; Shimakawa, Y.; Takano, M. *Trans. Mater. Res. Soc. Jpn.* **2006**, *31*, 41–46.
- Wang, J.; Neaton, J. B.; Zheng, H.; Nagarajan, V.; Ogale, S. B.; Liu, B.; Viehland, D.; Vaithyanathan, V.; Schlom, D. G.; Waghmare, U. V.; Spaldin, N. A.; Rabe, K. M.; Wuttig, M.; Ramesh, R. *Science* **2003**, *299*, 1719–1722.
- Niitaka, S.; Azuma, M.; Takano, M.; Nishibori, E.; Takata, M.; Sakata, M. *Solid State Ionics* **2004**, *172*, 557–559.
- Belik, A. A.; Iikubo, S.; Kodama, K.; Igawa, N.; Shamoto, S.; Niitaka, S.; Azuma, M.; Shimakawa, Y.; Takano, M.; Izumi, F.; Takayama-Muromachi, E. *Chem. Mater.* **2006**, *18*, 798–803.
- Kimura, T.; Kawamoto, S.; Yamada, I.; Azuma, M.; Takano, M.; Tokura, Y. *Phys. Rev. B* **2003**, *67*, 180401(R)-1–4.
- Azuma, M.; Takata, K.; Saito, T.; Ishiwata, S.; Shimakawa, Y.; Takano, M. *J. Am. Chem. Soc.* **2005**, *127*, 8889–8893.
- Ishiwata, S.; Azuma, M.; Takano, M.; Nishibori, E.; Takata, M.; Sakata, M.; Kato, K. *J. Mater. Chem.* **2002**, *12*, 3733–3737.
- Brown, I. D.; Altermatt, D. *Acta Crystallogr., Sect. B* **1985**, *41*, 244–247.

BiNiO_3 is an antiferromagnetic insulator with a Ni^{2+} -spin ordering temperature of 300 K at ambient pressure. The simple rock-salt-type oxide NiO , is known to be an antiferromagnetic charge transfer insulator. Although the Ni^{2+} /volume density is considerably higher for the latter material, BiNiO_3 shows a pressure-induced insulator to metal transition at a moderate pressure of 4 GPa²¹ while NiO does not metallize below 50 GPa.²² Synchrotron X-ray diffraction showed that the transition in BiNiO_3 is accompanied by a structural change to an orthorhombic GdFeO_3 -type perovskite superstructure, but it was not clear whether the transition involves melting of the Bi charge order ($\text{Bi}^{3+} + \text{Bi}^{5+} \rightarrow 2\text{Bi}^{4+}$) or whether some $\text{Ni} \rightarrow \text{Bi}$ charge transfer is also involved. To resolve this issue we have carried out a powder neutron diffraction study at high pressures to determine accurate atomic coordinates, from which the charge distribution in the HP phase is evident. In this article we show that the pressure-induced melting of the charge disproportionated state leads to a simultaneous charge transfer from Ni to Bi, so that the HP phase is metallic $\text{Bi}^{3+}\text{Ni}^{3+}\text{O}_3$.

2. Experimental Section

Polycrystalline BiNiO_3 was prepared at 6 GPa and 1000 °C with a cubic anvil type high pressure apparatus as reported previously.¹⁸ High-pressure time-of-flight (TOF) neutron diffraction patterns were recorded using the instrument PEARL/HiPr at the ISIS facility, U.K. About 90 mm³ of the sample was loaded into a Paris–Edinburgh cell²³ with 4:1 methanol–ethanol pressure medium and a small pellet of lead as the pressure calibrant. The cell was used in transverse geometry giving access to scattering angles $83^\circ < 2\theta < 97^\circ$. Rietveld profile refinements of the structural models were performed with the GSAS software.²⁴

3. Results and Discussion

TOF neutron diffraction data from BiNiO_3 collected at pressures up to 7.7 GPa on increasing the pressure are shown in Figure 1. Below 4 GPa, the diffraction patterns were similar to the ambient pressure (0.1 MPa) profile in Figure 1a. This has a $\sqrt{2}a_p \times \sqrt{2}a_p \times 2a_p$ superstructure, where a_p is the cubic perovskite lattice parameter, and triclinic $P\bar{1}$ symmetry. The refined structural model is consistent with that reported previously from synchrotron X-ray powder diffraction (refinement results and BVS calculations are given in Tables 1 and 2). A drastic change in the profiles is observed at pressures above 4 GPa, as shown in Figure 1b with the merging of peaks showing that the higher symmetry, orthorhombic, phase is formed. No phase coexistence was observed at 2.1 or 4.7 GPa, although this would be expected at pressures close to the first-order metal–insulator transition.

Refinements of the HP structure of BiNiO_3 gave good fits to the data assuming $Pbnm$ symmetry (Figure 1a), which characterizes the common GdFeO_3 -type perovskite superstructure. We also checked the possibilities of distorted GdFeO_3 type structures found in Bi and Ni containing perovskites, an acentric BiInO_3 -

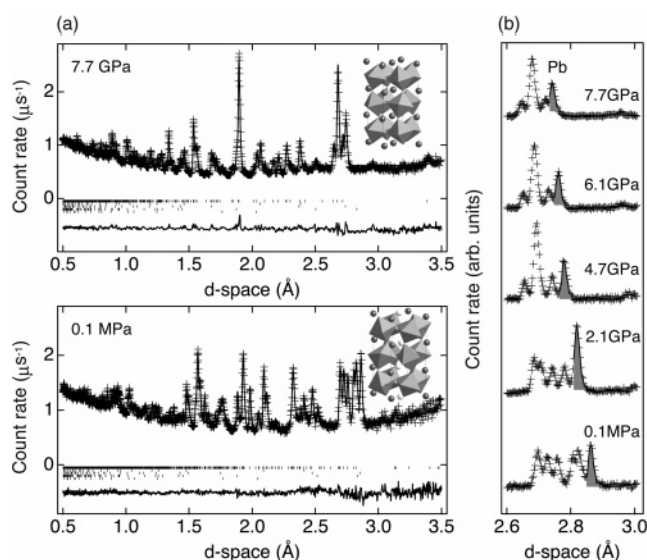


Figure 1. Time-of-flight powder neutron diffraction data for BiNiO_3 at variable pressures. (a) Rietveld fits of the triclinic structure to ambient pressure (0.1 MPa) data ($a = 5.3942(4)$ Å, $b = 5.6520(4)$ Å, $c = 7.7131(5)$ Å, $\alpha = 92.181(6)^\circ$, $\beta = 89.777(6)^\circ$, $\gamma = 91.704(5)^\circ$; fitting residuals; $\chi^2 = 1.779$, $R_{\text{WP}} = 0.0275$), and of the high pressure orthorhombic structure to 7.7 GPa data ($a = 5.2843(4)$ Å, $b = 5.4323(4)$ Å, $c = 7.5537(6)$ Å; $\chi^2 = 2.584$, $R_{\text{WP}} = 0.0359$). Observed (points), calculated (full line) and difference profiles are shown together with Bragg markers for the BiNiO_3 phase and secondary contributions (the sample consisted of 79.2 wt % BiNiO_3 , 3.6% NiO and 17.2 wt % Pb pressure standard; small contributions from WC and Ni in the anvils were also fitted). Insets show the ambient and high-pressure crystal structures, with dark and light spheres corresponding to Bi1 and Bi2 in the latter structure, respectively. (b) Selected data at various pressures showing the change in diffraction intensities around the 4 GPa insulator–metal transition, also a peak from the Pb pressure standard (shaded).

Table 1. Crystallographic Parameters for BiNiO_3 at 0.1 MPa and at 7.7 GPa

atom	site	x	y	z	$100 \times U_{\text{iso}} (\text{Å}^2)$
0.1 MPa ^a					
Bi1	2i	0.0037(14)	0.0452(11)	0.2324(9)	0.26(10)
Bi2	2i	0.5093(15)	0.4418(13)	0.7203(9)	0.26
Ni1	1d	0.5	0	0	0.33(6)
Ni2	1c	0	0.5	0	0.26
Ni3	1f	0.5	0	0.5	0.26
Ni4	1g	0	0.5	0.5	0.26
O1	2i	−0.1446(21)	0.4739(20)	0.2541(17)	0.6
O2	2i	0.3927(21)	0.0340(19)	0.7553(14)	0.6
O3	2i	0.8400(21)	0.1795(18)	−0.0303(14)	0.6
O4	2i	0.3200(21)	0.3293(19)	0.0862(16)	0.6
O5	2i	0.2207(21)	0.7687(16)	0.4099(15)	0.6
O6	2i	0.6609(18)	0.6836(16)	0.5467(12)	0.6
7.7 GPa ^b					
Bi	4c	−0.0052(15)	0.0470(6)	0.25	0.49(7)
Ni	4b	0.5	0	0	0.10(5)
O1	8d	0.7007(9)	0.2974(9)	0.0363(7)	0.78(6)
O2	4c	0.0870(13)	0.4840(13)	0.25	0.76(6)

^a Space group $P\bar{1}$, $a = 5.3942(4)$ Å, $b = 5.6519(4)$ Å, $c = 7.7131(5)$ Å, $\alpha = 92.182(7)^\circ$, $\beta = 89.780(7)^\circ$, $\gamma = 91.704(5)^\circ$, $\chi^2 = 1.812$, $R_{\text{WP}} = 0.0275$.

^b Space group $Pbnm$, $a = 5.2843(4)$ Å, $b = 5.4323(4)$ Å, $c = 7.5537(6)$ Å, $\chi^2 = 2.584$, $R_{\text{WP}} = 0.0359$.

- (20) Wadati, H.; Takizawa, M.; Tran, T. T.; Tanaka, K.; Mizokawa, T.; Fujimori, A.; Chikamatsu, A.; Kumigashira, H.; Oshima, M.; Ishiwata, S.; Azuma, M.; Takano, M. *Phys. Rev. B* **2005**, *72*, 155103–1–7.
- (21) Ishiwata, S.; M. Azuma, M.; Hanawa, M.; Moritomo, Y.; Ohishi, Y.; Kato, K.; Takata, M.; Nishihori, E.; Sakata, M.; Terasaki, I.; Takano, M. *Phys. Rev. B* **2005**, *72*, 045104–1–7.
- (22) Shukla, A.; Rueff, J. P.; Badro, J.; Vanko, G.; Mattila, A.; de Groot, F. M. F.; Sette, F. *Phys. Rev. B* **2003**, *67*, R081101–1–4.
- (23) Besson, J. M.; Nelmès, R. J.; Hamel, G.; Loveday, J. S.; Weill, G.; Hull, S. *Physica B* **1992**, *120*, 907–910.
- (24) Larson, A. C.; Von Dreele, R. B. *General Structural Analysis System (GSAS)*; Los Alamos National Laboratory Report; Los Alamos National Laboratory: Los Alamos, NM, 2000; pp 86–748.

type structure ($Pna2_1$) having ferroelectric Bi displacements,²⁵ and a Ni-charge disproportionated, monoclinic $P2_1/n$ YNiO_3 -type model,¹⁰ but the fits were not improved and the additional atomic displacements were negligible.

- (25) Belik, A. A.; Stefanovich, S. Y.; Lazoryak, B. I.; Takayama-Muromachi, E. *Chem. Mater.* **2006**, *18*, 1964–1968.

Table 2. Bond Valence Sums^a for BiNiO₃ at 0.1 MPa and at 7.7 GPa

	Bi1	Bi2	Ni1	Ni2	Ni3	Ni4
0.1 MPa	3.02	4.90	1.84	2.03	2.03	1.99
7.7 GPa	3.13		2.96			

^a $V_i = \sum_j S_{ij}$, $S_{ij} = \exp(r_0 - r_{ij}/0.37)$. Values calculated using $r_{ij} = 2.094$ for Bi³⁺, 2.06 for Bi⁵⁺, 1.67 for Ni²⁺, and 1.686 for Ni³⁺.

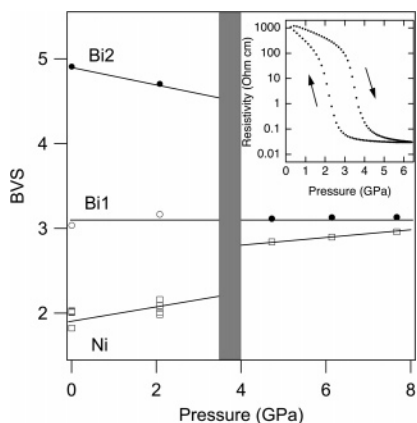


Figure 2. Bi and Ni bond valence sums (BVS) determined from the refined structures of BiNiO₃ at various pressures. The low-pressure structure contains two distinct Bi sites, labeled Bi1 (open circles) and Bi2 (filled circles), corresponding respectively to Bi³⁺ and Bi⁵⁺, and four Ni sites (squares) all containing Ni²⁺. The high-pressure structure contains single Bi (filled circles) and Ni (squares) sites, both with valences of 3+. The pressure region for the insulator-to-metal transition is shaded. The inset shows the resistivity of BiNiO₃ as a function of pressure exhibiting an insulator to metal transition at around 4 GPa. Details in the resistivity measurement are described in ref 21.

The charge distribution in the HP *Pbnm* phase of BiNiO₃ was investigated using bond valence sums and electronic structure calculations. The BVSs determined from the experimentally determined M–O distances using standard parameters²⁶ for M = Bi³⁺, Bi⁵⁺, Ni²⁺, and Ni³⁺ are shown in Figure 2. The BVSs for the ambient pressure phase confirm the Bi³⁺_{0.5}Bi⁵⁺_{0.5}Ni²⁺O₃ distribution, but a drastic change is observed above 4 GPa, where the BVSs for the single Bi and Ni sites in the HP phase are both very close to 3 (e.g., 3.13 and 2.96, respectively, at 7.7 GPa). This shows that the HP phase is Bi³⁺–Ni³⁺O₃, and hence that a complete one-electron Ni → Bi transfer has occurred at the insulator-to-metal transition.

Electronic structure calculations using the refined structural parameters support the above descriptions of the charge distributions in BiNiO₃. The electronic structure calculations were performed by the full-potential linearized augmented plane-wave (FLAPW) method using the augmented plane wave plus local orbitals (APW+lo) basis set based on density functional theory within the LDA+U approximation (where LDA is local density approximation and U is the on site Coulomb repulsion) in the WIEN2k package.²⁷ Coulomb and the exchange parameters, *U* and *J* were fixed to 8.0 and 0.95 eV, as commonly used in the calculations of Ni oxides.^{28,29} The G-type antiferromagnetic spin structure was assumed in the

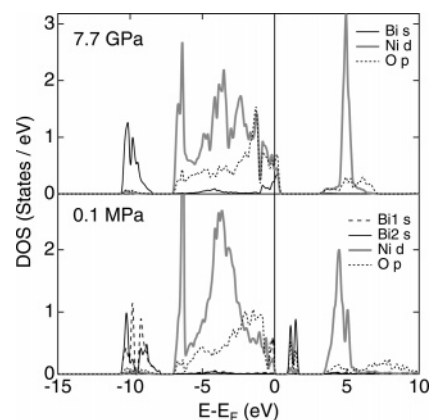


Figure 3. Electronic density-of-states (DOS) for BiNiO₃ calculated from the 0.1 MPa and 7.7 GPa structural data, with contributions from Bi 6s, Ni 3d, and O 2p states indicated. The ambient pressure phase (lower panel) shows the Bi charge-transfer gap expected for Bi³⁺_{0.5}Bi⁵⁺_{0.5}Ni²⁺O₃ whereas a substantial Ni 3d density-of-states is seen at the Fermi level for the metallic high-pressure Bi³⁺Ni³⁺O₃ phase (upper panel).

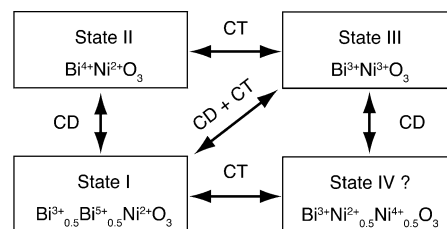


Figure 4. Electronic ground states for BiNiO₃ showing intermetallic charge transfer (CT) and charge disproportionation (CD) transitions. The pressure-induced CT accompanied with CD between states I and III is indicated.

calculations.³⁰ The atomic sphere radii RMT divided into two regions, non-overlapping atomic spheres and an interstitial region, are 2.5, 2.2, 2.0, and 1.6 au for Bi(7.7 GPa), Bi(0.1 MPa), Ni, and O. The cutoff (*K*_{max}) for the expansion of plane waves in the interstitial region was restricted by the relation on $RMT_{K_{max}} = 7$. In this study, we used 200 k points in the complete Brillouin zone for the all calculations. The density-of-states for the ambient pressure form as shown in Figure 3 exhibits a charge-transfer gap of 0.8 eV between lower and upper bands consisting respectively of Bi1 (Bi³⁺) and Bi2 (Bi⁵⁺) states, although both are strongly hybridized with O 2p states which reduces the cation charges. Although the DFT calculation tends to underestimate the gap size, this relatively narrow band gap is consistent with the value of 0.68 eV estimated from the electrical resistivity.¹⁸ By contrast, the density-of-states for the high-pressure Bi³⁺Ni³⁺O₃ phase confirm metallic character with the Ni d band predominantly crossing the Fermi level (as found in metallic La³⁺Ni³⁺O₃), and with no high-energy Bi band present, consistent with the Bi³⁺ ionic state.

Our results demonstrate that BiNiO₃ is a unique electronic material in having electronically variable A and B site cations, with an active intermetallic charge-transfer degree of freedom in addition to charge disproportionation instabilities at both the A and B sites. Four distinct electronic ground states can be adopted, as shown in Figure 4. Their stabilities are determined by the relative energies of the Bi 6s and Ni 3d levels, which are sensitive to lattice strain and so can be tuned by changes in

(26) Brese, N. E.; O’Keeffe, M. *Acta Crystallogr., Sect. B* **1991**, *47*, 192–197.
 (27) Blaha, P.; Schwarz K.; Madsen, G. K. H.; Kvasnicka, D.; Luitz, J. *WIEN2K, An Augmented Plane Wave Plus Local Orbitals Program for Calculating Crystal Properties*; Vienna University of Technology: Austria, 2001.
 (28) Anisimov, I. V.; Zaanen, J.; Andersen, O. K. *Phys. Rev. B* **1991**, *44*, 943–954.
 (29) Yamamoto, S.; Fujiwara, T. *J. Phys. Soc. Jpn.* **2002**, *71*, 1226–1229.

(30) The G-type antiferromagnetic spin structure was confirmed for the ambient pressure phase by a neutron diffraction experiment. This result will be published elsewhere.

temperature and pressure, or by chemical doping. Bi^{4+} charge disproportionation stabilizes the observed ambient state I of BiNiO_3 . State II, $\text{Bi}^{4+}\text{Ni}^{2+}\text{O}_3$, has not been observed below the decomposition temperature in pure BiNiO_3 , but disorder induced by Pb-doping disrupts the long-range $\text{Bi}^{3+}/\text{Bi}^{5+}$ charge order resulting in a substituted form of ground-state II, $\text{Bi}^{4+}_{0.8}\text{Pb}^{4+}_{0.2}\text{Ni}^{2+}\text{O}_3$.³¹ The Bi^{4+} oxidation state was also confirmed by core-level photoemission in the La-doped compound, $\text{Bi}^{4+}_{1-x}\text{La}^{3+}_x\text{Ni}^{(2+x)+}\text{O}_3$,^{20,21} where the hole-doping of Ni ions makes the system metallic. Our present study demonstrates that a different band metallic state III, $\text{Bi}^{3+}\text{Ni}^{3+}\text{O}_3$, is produced by pressure-induced charge transfer. This is not accompanied by disproportionation of the resulting Ni^{3+} ions although the latter instability is also sensitive to lattice effects and occurs in RNiO_3 for R^{3+} 's smaller than La^{3+} or Bi^{3+} . Hence, we predict that the Ni-disproportionated ground state IV, $\text{Bi}^{3+}\text{Ni}^{2+}_{0.5}\text{Ni}^{4+}_{0.5}\text{O}_3$, should be stabilized at high pressures and low temperatures in the pure material or in substituted $\text{Bi}^{3+}_{1-x}\text{R}^{3+}_x\text{Ni}^{2+}_{0.5}\text{Ni}^{4+}_{0.5}\text{O}_3$ for small R^{3+} ; this will be investigated in future studies.

In conclusion, we have shown that a variety of electronic ground states are possible in the perovskite BiNiO_3 because of competing intermetallic and disproportionation charge instabili-

ties. The pressure-induced insulator to metal transition occurs via an unprecedented simultaneous melting of Bi-charge disproportionation and $\text{Ni} \rightarrow \text{Bi}$ charge transfer; $\text{Bi}^{3+}_{0.5}\text{Bi}^{5+}_{0.5}\text{Ni}^{2+}\text{O}_3 \rightarrow \text{Bi}^{3+}\text{Ni}^{3+}\text{O}_3$. A further ground state is stabilized by Pb- or La-substitutions, and we predict that a fourth Ni-disproportionated state should be observable at high pressures and low temperatures or through other lanthanide substitutions. The multiple electronic instabilities in BiNiO_3 may offer new possibilities for tuning electronic phenomena in oxides and creating devices based on switching between the different phases as have been demonstrated for perovskite manganites.

Acknowledgment. The authors express their thanks to Prof. Tamio Oguchi for fruitful discussion and the help in electronic structure calculations. This work was supported by the Ministry of Education, Culture, Sports, Science and Technology, Japan Grants-in-Aid No. 17105002 and 18350097. We also thank the Leverhulme Trust and EPSRC for financial support and the provision of neutron beamtime.

Supporting Information Available: Bi–O and Ni–O bond lengths at selected pressures. This material is available free of charge via the Internet at <http://pubs.acs.org>.

JA074880U

(31) Ishiwata, S.; Azuma, M.; Takano, M. *Chem. Mater.* **2007**, *19*, 1964–1967.